Implementation and Verification of a Wave-to-Wire Model of an Oscillating Water Column with Impulse Turbine

J. F. Kelly[1a], W. M. D. Wright[1b], W. Sheng[2], K. O'Sullivan[3]

[1] *Department of Electrical and Electronic Engineering, University College Cork, College Road, Cork, Ireland*

[2]*MaREI, Environmental Research Institute, University College Cork, Cork, Ireland*

[3]*Marine Energy Engineer, Black & Veatch Ltd., Grosvenor House, 69 London Road, Surrey, RH1 1LQ, UK*

[a]james.kelly@ucc.ie, [b]bill.wright@ucc.ie

***Abstract*—The increased demand for clean renewable sources of electricity has fostered strong growth in wave energy development in recent years. This led to greater understanding of the various systems involved in the conversion of wave energy to electrical energy, which in turn led to more accurate and sophisticated models of each system. Mathematical models have been developed independently to represent the various interactions that take place within wave energy converters (WEC). In this paper, models used to represent the various stages of energy conversion that occur within an oscillating water column (OWC) have been combined to create a single wave-to-wire model of an OWC. The model was then compared to the experimental results from the FP-7 CORES OWC deployment project. The results show good agreement between modelled and experimental data. The model can be used to estimate the power output of an OWC, as well to test control strategies and algorithms allowing for development in the control of OWCs before physical deployment.**

***Index Terms*—impulse turbine, ocean energy, oscillating water column, renewable energy, wave energy, wave-to-wire model**

I. Introduction

The demand for renewable sources of energy has been growing in recent years, with an emphasis on finding new, reliable sources of energy to complement the wind energy sector. One area that has seen an increase in attention and development has been Wave Energy Converters (WEC). One of the most advanced WEC technologies is the Oscillating Water Column (OWC) [1]. Large-scale bottom-fixed shoreline OWCs, such as LIMPET in Scotland [2], Pico OWC in Azures, Portugal [3], and the Mutriku plant in Spain [4], have been successfully connected to power grids. Floating offshore OWCs have also been developed and investigated [5, 6], as they have a much higher potential for total power extraction [7].

A floating OWC uses a four-step process to convert wave energy into electrical power: 1) energy in propagating sea waves is converted to kinematic energy by the motions of the OWC, 2) the kinematic energy is converted into pneumatic energy through a thermodynamic process that depends on the Power Take-Off (PTO) system damping of the turbine, 3) the pneumatic energy in the air flow is converted into rotating mechanical energy by the air turbine, 4) the mechanical energy is converted into electrical energy by a generator and a controller. Each step in this conversion has been individually and independently modelled, yet the models are interdependent and relatively complex [8-15].

Wave-to-wire models for a point absorber type WECs operating in irregular seas have recently been developed [16, 17], and the aim of the work presented in this paper is to create a single wave-to-wire model for an OWC in irregular seas by combining the individual models of each step in the OWC conversion process. The model was then verified using experimental data from open sea device deployment. The single model can be used to estimate both instantaneous and average mechanical and electrical power output given an irregular wave state array and can be used to test control strategies to improve device performance prior to deployment. The oscillating nature of the instantaneous power output of WECs can affect power quality [18]. Attempts at mitigating the poor power quality produced by offshore OWCs have been investigated in [19, 20], and being able to model instantaneous device behaviour is advantageous. The hydrodynamic modelling, turbine modelling, and controller modelling are all very design dependent, and each model can be easily modified to match any design criteria. For verification and validation, the model presented here was compared with the experimental results of the FP-7 Components for Ocean Renewable Energy Systems (CORES) project that was completed in 2011 [21].

The CORES OWC consisted of a Bent Backwards Duct Buoy (BBDB) that had an impulse turbine with a diameter of 677 mm and active moving guide vanes upstream and downstream. The turbine was housed in a duct with a bell-shaped opening on either end, along with the electrical generator that had a rated speed of 769 rpm and a rated power output of 11 kW [21]. The numerical models presented were created to represent the components of the CORES system.

II. Numerical Modelling

A. Hydrodynamics

Modelling the conversion of wave motion to electrical energy by an OWC requires finding the motion of the Internal Water Surface (IWS) in response to the changing elevation of the ocean surface. The IWS acts like a piston and forces air across a turbine, which is the mechanical PTO of the system. Therefore, the first step is to model the motion of the IWS in a given wave climate. Recent publications, including [10, 11], have explored how the hydrodynamics of the OWC can be reliably modelled.

A BBDB OWC is modelled in this paper and is shown in Fig. 1. The modelling of the IWS inside the BBDB is calculated using a Boundary Element Method (BEM) solver to find the pressure distribution implicitly, as presented in [22, 23]. The implicit calculations solved with the BEM using reciprocity

relations to find the IWS parameters from the oscillating structure were introduced in [24]. The implicit calculations were performed on the BBDB model using linearized frequency domain numerical modelling, carried out by the industry standard commercial code WAMIT v6.4. The hydrodynamic terms related to the IWS movement, including air-pressure fluctuations, can all be obtained from potential flow code without explicitly solving for the radiation potential of the internal water surface using WAMIT v6.4 [25]. Hence, the resulting air flow calculated from the IWS includes both the excitation and radiation flows. The verification of this process is given in detail in [11].

Frequency domain modelling was employed to determine the motion response amplitude operators (RAO) of the BBDB. The analysis was restricted to head seas, as performance of the OWC in head seas is assumed to be more efficient. During modelling, the surge, heave, pitch and IWS RAO's were determined for the BBDB and presented in [8].

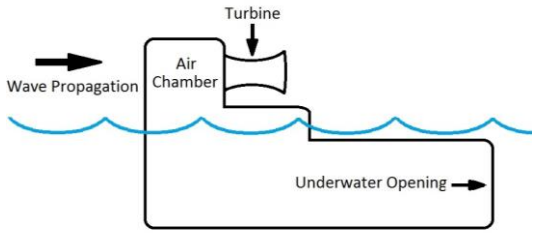

Fig. 1: Example of a Bent Backwards Duct Buoy OWC.

The resonance period of the IWS RAO plots produced by the WAMIT simulations are illustrated in Fig. 2. The most common periods at SEAI test site in Galway Bay where the CORES buoy was deployed fall between 2.5 s and 6.5 s [26], which corresponds to the maximum RAO as shown in Fig. 2. This was designed intentionally to extract the maximum energy from the resource [27].

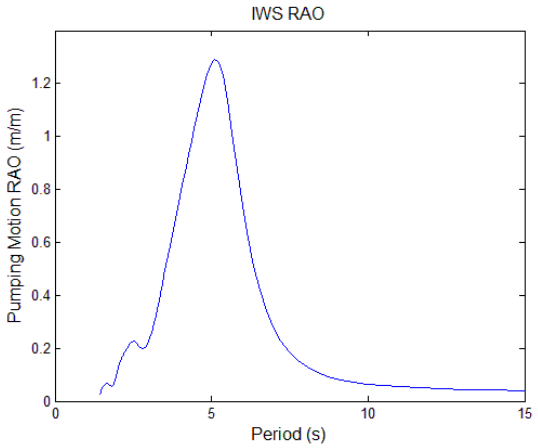

Fig. 2: Internal Water Surface Response Amplitude Operators.

In order to validate these predictions made by WAMIT and the empirical damping applied from various sources, a basic tank 1/50 scale testing campaign was undertaken using the device configuration for the BBDB. The model testing was performed and verified in the wave flume at National Ocean Test Facility (formerly HMRC), University College Cork, Ireland [8]. The plot in Fig. 2 was established by taking the FFT from the WAMIT simulations. Due to the limitations of crossing from the discrete domain to the time domain, the RAO response is limited to simulating seas with a significant wave height, H_s, of 4 m and below.

The verified RAO of the IWS was then used in conjunction with a randomized sea state based on the Bretschneider spectrum to model the IWS movement in the BBDB in various sea conditions. The Bretschneider spectrum is one of several parametric functions commonly used to approximate spectral densities for engineering and design purposes, and it is derived from statistical analysis of large databases. Unimodal forms of parametric functions are limited because they cannot allow for an accurate depiction of complex sea-states [28].

The Bretschneider sea state was created in MATLAB using the values for the significant wave height and significant period of the desired conditions. To generate the ocean waves, a multitude of sinusoidal wave forms in the time domain were created based on the Bretschneider spectral density. Each sinusoidal wave had a different frequency and a random phase shift; the wave forms were superimposed upon each other to produce a single array that represented the height of the water level at the device. To find the water level within the chamber based on the generated waves, the amplitude of each sinusoidal component of the array was multiplied by the RAO value that corresponded to the sinusoidal wave period. The results from the RAO multiplier were superimposed upon each other to produce an array that represented the water level of the IWS.

B. Thermodynamics

The thermodynamics of the air in an OWC chamber has not been as thoroughly researched as the hydrodynamics [29]. The compressibility of a large volume of air in OWC operation was originally presented in [30], and it has been used in time-domain modelling in [31]. The air flow across the turbine is driven by the change in volume of the air chamber, which is dictated by the movement of the IWS. Equation (1) is the differential equation used to represent the change of mass within the air chamber, while (2) is the flow rate calculated from the movement of the IWS [32].

$$\frac{dm}{dt} = \rho_c \frac{dV}{dt} + V \frac{d\rho_c}{dt}, \tag{1}$$

$$Q_w = -\frac{dV}{dt}, \tag{2}$$

where m is the mass of air in the chamber, ρ_c is the density of air inside the chamber, V is the volume of air inside the chamber, and Q_w is air flow as calculated by the change in volume because of the IWS motion. The change of volume is based on the static radiation admittance used in the WAMIT simulations, which has a value in SI units of $m^3s^{-1}Pa^{-1}$ and is the inverse of aerodynamic damping [24].

Due to the compressibility of air and the need to account for the changing density of the air flow across the turbine, separate thermodynamic equations were used: one for inhalation when the chamber pressure is lower than atmospheric pressure, and one for exhalation when the chamber pressure is higher than atmospheric pressure, as shown in (3):

$$\begin{cases} Q_p = -\frac{1}{\rho_c}\frac{dm}{dt}, p \geq 0, \\ Q_p = -\frac{1}{\rho_0}\frac{dm}{dt}, p < 0, \end{cases} \tag{3}$$

where p is the gauge pressure of the OWC chamber and Q_p is the air flow across the turbine. In exhalation, the air within the chamber is essentially a single entity that remains uniform in terms of its thermodynamic behaviour. However, during inhalation, the residual air inside the chamber goes through a complex mixing process with the air induced from the atmosphere. To simplify the mathematical model of this process, the mixing can be considered to be instantaneous [33], and thus the air within the chamber is assumed homogenous and isentropic during both inhalation and exhalation. With these assumptions, the air can be expressed by the uniformity parameters, including pressure, density, and temperature, and the volumetric flow of the air across the turbine in an OWC can be written as:

$$\begin{cases} Q_p = Q_w - \frac{V}{\gamma p_0 + p}\frac{dp}{dt}, p \geq 0, \\ Q_p = \left(1 + \frac{p}{\gamma p_0}\right) Q_w - \frac{V}{\gamma p_0}\frac{dp}{dt}, p < 0, \end{cases} \quad (4)$$

where p_0 is the air pressure at atmospheric conditions and γ is the specific heat ratio of air and has a value of 1.4. The impulse turbine, which is used in this model, operates as a nonlinear PTO. The pressure drop across the turbine can be approximated using a second order polynomial of the flow rate, as shown in (5) [33],

$$\begin{cases} p = kQ_p^2, p \geq 0, \\ p = -kQ_p^2, p < 0, \end{cases} \quad (5)$$

where k is the damping coefficient of the turbine, which is given in SI units of Pa $m^{-6}s^{-2}$ and is related to the radiation admittance of the turbine. Combining (4) and (5) yields:

$$\begin{cases} \frac{dV}{dt} + \frac{V}{\gamma p_0 + p}\frac{dp}{dt} + \sqrt{p/k} = 0, p \geq 0, \\ \left(1 + \frac{p}{\gamma p_0}\right)\frac{dV}{dt} + \frac{V}{\gamma p_0}\frac{dp}{dt} - \sqrt{-p/k} = 0, p < 0. \end{cases} \quad (6)$$

Equation (6) represents the relationship between the chamber pressure and the air volume for a nonlinear PTO. If pressure, p, or volume, V, is known, the other can be found using this equation. Once both values are known, the flow across the turbine can be calculated if k is known.

C. Impulse Turbine

The self-rectifying impulse turbine has become more widely considered for the OWC due to its non-stall feature and better efficiency at high flow rates. Studies have been carried out to characterise the turbine through laboratory testing and Computational Fluid Dynamics simulation. Equations (7-10) published in [34, 35] can be used at any scale to characterise the turbine and can be used in turbine design.

$$\phi = \frac{v_a}{U_R}, \quad (7)$$

$$C_t = T_o/\{\rho_a(v_a^2 + U_R^2)bl_r z r_R/2\}, \quad (8)$$

$$C_a = \Delta pQ/\{\rho_a(v_a^2 + U_R^2)bl_r z v_a/2\}, \quad (9)$$

$$\eta = \frac{(T\omega)}{(\Delta pQ)} = \frac{C_t}{(C_a\phi)}. \quad (10)$$

Here, ϕ is the flow coefficient, v_a is the velocity of air at the turbine, U_R is the blade linear velocity at the mid-span of the turbine blade, C_t is the torque coefficient, T_o is the torque, b is the blade height, l_r is the blade chord length, z is the number of blades, r_R is the turbine mean radius, C_a is the input power coefficient, η is the efficiency of the turbine, and ω is the rotational velocity of the turbine.

These non-dimensional equations may be used to determine the turbine characteristics in terms of expected performance under steady flow conditions. They depend on the Reynolds number, chord length, axial flow velocity, and several other values that lead to complex unit-dependent parameters. However, dimensionless analyses have shown that at flow velocities where the effects of the Mach number and Reynolds number are negligible, characterising turbine performance can be done using non-dimensional parameters that are functions of only the flow coefficient [12].

The turbine performance depends on the rotational speed of the turbine, the volumetric flow rate, the density of the air, and the diameter of the turbine. With these values, the most important performance characteristics, mechanical power, pressure drop across the turbine, and pneumatic to mechanical power conversion efficiency can be found using the following simplified non-dimensional functions [35] of the flow coefficient:

$$\Phi = \frac{Q_p}{(\omega D^3)}, \quad (11)$$

$$\Psi = \frac{P_m}{(\rho\omega^3 D^5)} = f(\Phi), \quad (12)$$

$$\Upsilon = \frac{\Delta p}{(\rho\omega^2 D^2)} = g(\Phi), \quad (13)$$

$$H = \frac{P_m}{\Delta pQ} = \frac{\Psi}{\Upsilon\Phi} = h(\Phi), \quad (14)$$

where ω is the rotational speed, Q is the flow rate across the turbine, ρ is the density of air, D is the diameter of the turbine, Δp is the pressure drop across the turbine, P_m is the mechanical power, Φ is the flow coefficient, Ψ is the torque coefficient, Y is the input pressure coefficient, and H is the efficiency of the turbine.

Substitution may be used to show the direct relationship between ϕ and Φ. These two equivalent quantities only differ by a constant multiplier that is related to the hub-to-tip ratio, ξ, and hence they can be used interchangeably to determine the behaviour of the turbine. Equations (15-16) express U_R, v_a, and ϕ in terms of Q_p, ω, D, and ξ, and thus show that (11-14) may be used in place of (7-10).

$$U_R = \frac{\omega D(1+\xi)}{4}, v_a = \frac{4Q_p}{\pi D^2(1+\xi)(1-\xi)}, \quad (15)$$

$$\phi = \frac{Q_p}{\omega D^3}\left\{\frac{16}{\pi(1+\xi)^2(1-\xi)}\right\}. \quad (16)$$

Equations (12-14) are polynomial functions of Φ and are typically found experimentally. Once these functions are known, the turbine can be mathematically modelled, and the model can be used to predict turbine performance. The coefficients used for the turbine were determined experimentally though laboratory testing.

D. Full Model

By combining the techniques described previously, a complete wave-to-wire model of an OWC in the time domain was created in SIMULINK, and this model has shown good correlation with the real observations from the CORES deployment in 2011. This single wave-to-wire model was constructed by finding the interdependent variables between the four independent modelling steps and linking them to create the most accurate complete model possible. The primary co-dependent variable for the full system is the radiation admittance or aerodynamic damping of the system produced by the turbine. It affects the pressure within the air chamber and the volumetric flow across the turbine, and the variation of the air pressure in the chamber affects the movement of the IWS. The flow chart in Fig. 3 illustrates how the full model works.

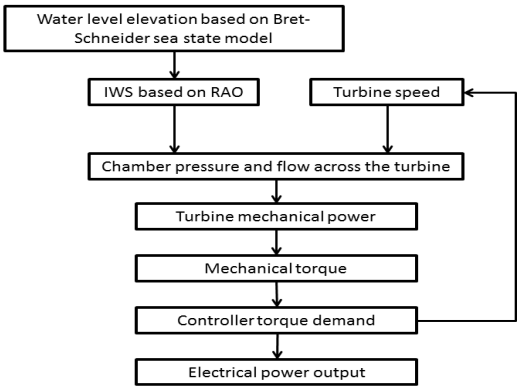

Fig. 3: Model flow chart

The effects of the turbine damping on the IWS movement and flow across the turbine are difficult to quantify and often the pneumatic damping in OWC models is taken as constant [36] or ignored [37]. As the WAMIT model could not be directly coupled to the SIMULINK model, the changes in the radiation admittance caused by the turbine damping could not be directly applied to the movement of the IWS, and the pneumatic damping is taken as a constant for the hydrodynamic model. To address the turbine damping inconsistency within the model presented here, the volumetric flow produced by the IWS motion was used along with the rotational speed of the turbine to find the flow coefficient based on Q_w, which was then used to approximate the damping coefficient of the turbine. The damping coefficient of the turbine, k, was calculated from the second order polynomial function of the flow coefficient that is determined experimentally using:

$$k = \frac{\Delta p}{Q_w^2} = k(\Phi). \tag{17}$$

The calculated value of k is then used in (5) to determine the change in pressure over the sample time. With the new pressure value calculated, the damping coefficient is used to determine the value of Q_p, which is then used with (11-14) to approximate the behaviour of the impulse turbine. The mechanical torque applied to the turbine by the calculated flow is combined with the electrical braking torque applied by the generator to determine the changing rotational speed of the turbine. The estimated speed of the turbine is then used to adjust the electrical torque demand as dictated by the controller. The electrical braking torque is combined with the rotational speed of the turbine to determine the electrical power output of the system. By calculating Q_p based on the turbine damping and applying that flow to the turbine model rather than using the flow calculated directly from the hydrodynamic system, the model acts to mitigate the limitations inherent to the indirectly coupled hydrodynamic system.

III. Results and Discussion

The turbine model depends on the output of the thermodynamic model, while the thermodynamic model has inputs from both the turbine speed and the change in chamber volume caused by the hydrodynamic action of the buoy. Thus, the full model was verified against the CORES data in reverse order to minimize the complexity during the verification process, i.e. the turbine model was verified first, followed by the thermodynamic model, and finally the hydrodynamic model. This allowed for simpler troubleshooting of the model during development because the accuracy of each stage could be confirmed separately and any inconsistencies in further tests could be attributed to a given area. There were 8 operational periods that spanned between 9 and 43 minutes in duration, totalling approximately 3 hours of experimental data. The three comparison points for experimental versus modelled data were mechanical power, electrical power, and rotational velocity of the turbine.

A. Turbine Model

The turbine and controller model was verified by inputting flow calculated from the CORES data using the Bernoulli method presented in [38]. Flow data from the 8 cases were used in place of the output from the thermodynamic model.

The experimental data representing the mechanical power and rotational velocity of the turbine acquired during the CORES deployment were used to calculate mechanical torque. The mechanical power was calculated using electrical power, frictional losses, and inertia of the system. This was done as in [38] using:

$$P_m = P_e + B\omega^2 + J\omega\frac{d\omega}{dt} \tag{18}$$

where P_m is mechanical power, P_e is the measured electrical power, B is the frictional power loss, and J is the inertia of the turbine.

For the model, the instantaneous mechanical torque applied to the turbine is calculated using (12) and the rotational velocity of the turbine. The change in the rotational velocity of the turbine is inferred by combining the mechanical torque with frictional losses, turbine inertia, and electrical braking torque applied by the controller, as given by:

$$\frac{d\omega}{dt} = \frac{T_m - T_e - T_f}{J} \tag{19}$$

where T_m is the mechanical torque of the turbine, T_e is the electrical braking torque from the generator, and T_f is the braking torque due to friction.

Control laws were used to determine the braking torque from the rotational velocity of the turbine. The control laws used were based on a torque-speed curve that was designed to

optimise power quality without compromising system efficiency. The torque-speed curves used during CORES testing were made up of third-order polynomials in which the speed in rpm was the input and the torque to be applied was the output, given by [21, 38] as:

$$T_{ref} = K_{13}n^3 + K_{12}n^2 + K_{11}n + K_{10}, \quad (20)$$

where T_{ref} is the braking torque reference, n is the speed of the turbine in rpm, and K_{1x} are the control law coefficients.

The coefficients for the third-order controller used in the model were found by plotting the real torque reference against the rotational velocity and using a curve fit to match the data. For each production data set, the control law coefficients changed, requiring a new curve fit for each simulation. If the control algorithms present in the model were not adjusted to match the algorithms used experimentally, the modelled data were found to be inaccurate. The necessity of adjusting the turbine speed controller illustrated that the model could be trusted when testing turbine control methods. Table I shows the R^2 values of the curve fits used to determine the control law coefficients, and the total time duration of each of the 8 samples analysed. The longer the duration of the data sample, the less accurate the controller coefficients found using the curve fitting method.

Sea State		Controller Curve Fit	Duration of Sample
Hs	*Tz*	R^2 Value	(min)
1.22	3.96	0.6668	43
1.26	3.53	0.9947	9
1.44	3.80	0.985	12
1.09	3.57	0.9995	10
1.09	3.57	0.9947	11
1.28	3.65	0.9228	17
1.68	4.43	0.7967	35
1.64	4.45	0.6545	31

Table I: R^2 values for the curve fits used to determine the control law coefficients and the duration of data collected for each sample.

When modelled and experimental values for total average mechanical power, electrical power, and rotational velocity were compared, modelled values were within 4.6%, 3.7% and 0.1% of experimental values, respectively. Modelled and experimental data therefore showed respectable agreement, despite numerous potential sources for discrepancy. These sources included differences in the sea conditions, the calculations of flow and mechanical power from the CORES data, and the curve fitting used to find the third-order polynomials used by the torque controller.

Table II shows the average experimental and modelled electrical power and turbine rotational velocity for the 8 periods of operation used for model validation. In all periods of operation, the modelled data agree well with the experimental data from the CORES testing. The power output of the model was slightly higher than the experimental results in 7 out of the 8 sea states.

Sea State		Electrical Power (W)			Rotational Velocity (rpm)		
Hs	*Tz*	Model	Actual	Error	Model	Actual	Error
1.22	3.96	1510.5	1447.6	4.3%	343.5	361.6	-5.0%
1.26	3.53	2969.2	3051.1	-2.6%	607.7	603.5	0.7%
1.44	3.80	2368.7	2316.8	2.24%	391.9	396.3	-1.1%
1.09	3.57	2212.1	2141.0	3.3%	555.6	537.8	3.3%
1.09	3.57	2153.2	2047.8	5.1%	503.7	494.8	1.8%
1.28	3.65	2476.2	2353.2	5.2%	372.2	386.1	-3.6%
1.68	4.43	2247.5	2023.4	11.0%	323.3	312.8	3.3%
1.64	4.45	2040.2	1957.2	4.2%	310.2	312.3	-0.6%
Total		2247.2	2167.3	3.6%	426.0	425.7	0.1%

Table II: Experimental and modelled average electrical power and average rotational velocity outputs based on real flow conditions.

The coefficients of the control algorithm used over the individual samples affected the operating speeds of the turbine in the various simulations. This demonstrates that the modelled results are ideal for verifying the effectiveness of the control algorithms. The differences caused by the control algorithms can be seen in both the average rotational velocity of the turbine and the power outputs, where power output increases at the higher rotational velocity.

B. Thermodynamic Model

With the turbine model validated, the thermodynamic model's accuracy in estimating the flow across the turbine could be validated using the CORES data in a similar manner. Any discrepancies in the results could be traced back to the thermodynamic model because the turbine model was shown to be accurate. The thermodynamic model validation relies on (12) and (19) to infer mechanical torque and rotational speed of the turbine, and the data from the same 8 periods of operation were used in the validation process. However, the flow input for the turbine model during these tests of the thermodynamic model was calculated using (1-6).

To perform the calculations necessary to find the flow across the turbine, the change in volume of the inner chamber of the OWC was calculated from the experimental data. It was based on the changing elevation of the IWS. The IWS motion from the CORES project was calculated from the flow used in the turbine model verification, the known surface area of the IWS, and the gauge pressure in the inner chamber of the OWC. The gauge pressure inside of the chamber allowed the determination of the flow direction and therefore the direction of the IWS movement. This was accomplished using:

$$h_I(i) = \left[{Q_C}/{A} * sign(p)\right] + h_I(i-1), \quad (21)$$

where h_I is the height of the IWS, Q_C is the flow calculated from the original CORES data, and A is the area of the IWS of the OWC.

The overall difference between modelled and experimental values of the average mechanical power, electrical power, and rotational velocity were 6.1%, 4.5%, and 0.9%, respectively. The differences were greater than the turbine-only model, but that result was expected as more uncertainty was introduced by using the IWS values calculated with (21).

Figs. 4 and 5 are a sample-to-sample comparison of experimental data against the turbine-only and turbine-thermodynamic models from the 43-minute operational period. It can be seen that the modelled data followed the experimental data well. Fig. 4a shows the rotational velocity of the turbine while Fig. 4b shows the braking torque demand, which is determined by (20). Both sets of modelled data for the rotational velocity of the turbine were slightly lower than the experimental, while the braking torque demand was slightly higher. This was likely caused by a small difference in the coefficients of the torque reference polynomial. These results were not unexpected because of how the coefficients used in the

model were found and the R^2 value of the curve fit; the error was within an acceptable range.

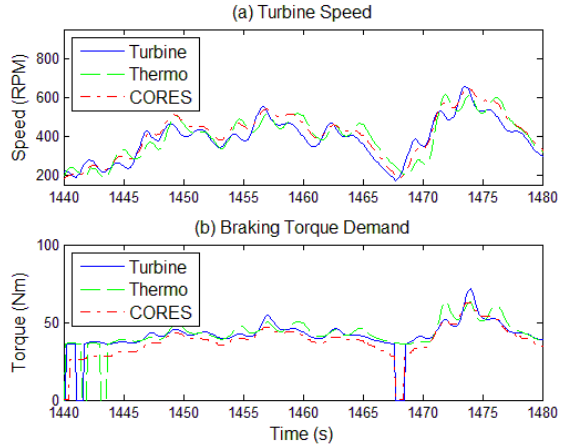

Fig. 4: Rotational speed and braking torque demand from experimental (CORES), turbine-only model (Turbine), and turbine-thermodynamic model (Thermo) during a sea state where H_s = 1.22 and T_z = 3.96.

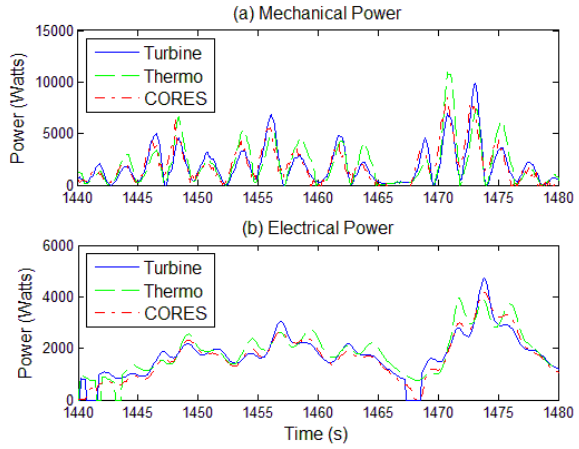

Fig. 5: Mechanical (a) and electrical (b) power output from experimental (CORES), turbine-only model (Turbine), and turbine-thermodynamic model (Thermo) during a sea state where H_s = 1.22 and T_z = 3.96.

Fig. 5a presents the mechanical power output and Fig. 5b presents the electrical power output of the experimental data along with the output data from the turbine-only and the turbine-thermodynamic models from the same sample and over the same time period shown in Fig. 4. Again, the plots show good agreement between the modelled and experimental data and are representative of all 8 operational periods. These results show that the numerical models used to represent the turbine and the electrical controller are accurate, reliable models that can be used for the PTO.

The thermodynamic tests show good agreement between modelled and experimental data but have more inconsistencies than the results of the turbine-only model. These differences can be attributed to the flow calculated using the thermodynamic equations presented earlier and that the IWS movement had to be inferred from the available data. Fig. 6 plots the model calculated flow and the experimental flow for the same time frame as in the previous figures. The root-mean square values of the modelled flow and experimental flow over the entire 43-minute sample are 2.7112 m^3s^{-1} and 2.7049 m^3s^{-1}, which results in a difference of ~0.2%. Similar results in modelled flow versus experimental flow were found in all 8 tested operational periods, with difference ranging from ~0.2% to ~4.3%.

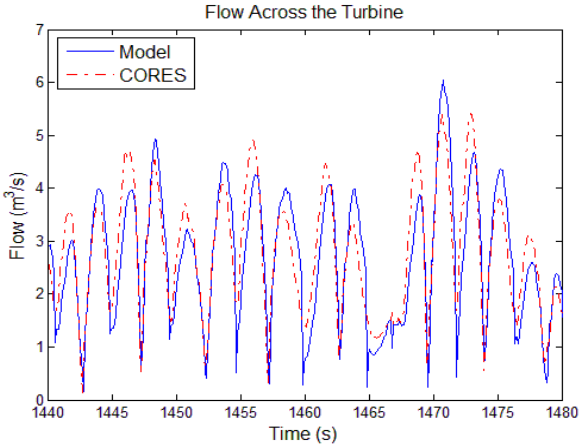

Fig. 6: Modelled and experimental (CORES) flow across the turbine during a sea state where H_s = 1.22 and T_z = 3.96.

C. *Hydrodynamic Model*

With the turbine and thermodynamic models both validated, the hydrodynamic model was tested against the CORES data. However, validating the hydrodynamic model of the OWC by comparing it to the experimental data was more difficult. When verifying the turbine and thermodynamic models, experimental data arrays were available as inputs to the models, allowing for easy and accurate comparisons of model versus experimental data.

For the hydrodynamic model, only the summary statistics of the sea states analysed were available, so wave arrays were created with MATLAB by using a Bretschneider spectrum to model the motion of the sea water surface in a predetermined sea state. The hydrodynamic model combined with the Bretschneider spectra did not perform as favourably as the turbine and thermodynamic models when compared to the experimental data. The modelled and experimental average mechanical power and electrical power outputs did not match well, as the model results always being higher than the experimental. The flow rates associated with the IWS motion created by the hydrodynamic model reached up to 12 m^3s^{-1}. The maximum flow rates seen in the experimental data were approximately 7 m^3s^{-1}. At pressures over 5,000 Pa, a difference of 1 m^3s^{-1} in flow relates to a 5 kW difference in pneumatic power, so the higher flows seen in the model substantially affected the modelled power output.

The failure of the hydrodynamic model to match the experimental data was traced to two main sources. A study of the spectral data at Arch Point from Section 7 in [27] found that the average of the spectra recorded over a month or longer shows good agreement with the Bretschneider spectrum. However, this agreement between average recorded spectra and the Bretschneinder spectra breaks down as time averaging scales are reduced to durations of a single day or less. The longest continuous data set from the CORES deployment was less than two hours in duration, making it unlikely that the hydrodynamic model output would match the experimental data.

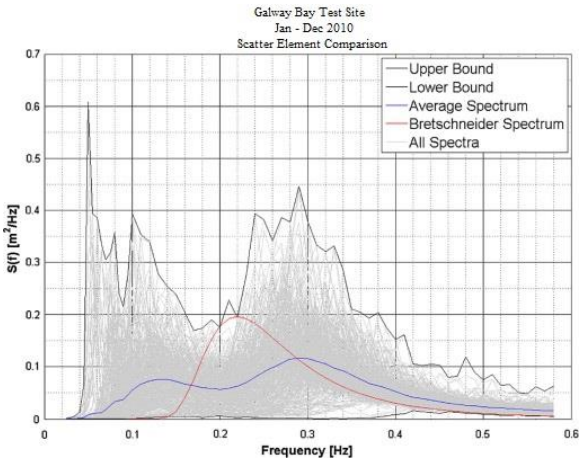

Fig. 7: Individual, averaged, and theoretical spectra within the ranges 0.625 m < H_s < 0.75 m and 3.0 s < T_z < 3.5 s for the Galway Bay test site [26].

Additionally, the average spectrum at the Galway Bay test site does not match the common parametric functions used to approximate spectral data because the wave conditions at the site are influenced by both local wind conditions and swell conditions in the North Atlantic [26]. Fig. 7 presents individual and averaged spectra measured at the Galway Bay test site for a given sea state measured over a 12 month period, along with the Bretschneider spectrum under the same conditions. The peak frequency occurrence in the Bretschneider spectrum corresponds with a lull in frequency occurrence in the average spectrum, thus making the Bretschneider spectrum a poor substitute for sea conditions in Galway Bay. To properly evaluate the hydrodynamic model, months of operational data from an open ocean site similar to the SEAI Belmullet test site, where the average spectrum matches the Bretschneider spectrum, would be required to avoid the failure points observed in the verification attempts presented in this paper.

IV. Conclusion

The combined single wave-to-wire model was shown to produce accurate representations of the OWC system as a whole. The turbine modelling showed good agreement with experimental results of open sea testing, the generator and turbine controllers were accurately and effectively tested, and the thermodynamic modelling of air flow and pressure was accurate. Turbine speed feedback was used to adjust the pneumatic damping of the system. However, the hydrodynamic modelling based on artificially generated Bretschneinder wave spectra and WAMIT RAO requires further varification.

The model presented in this paper could be used for testing and evaluating various components of an OWC. The model allows the development and testing of control algorithms to help further improve the efficiency of OWCs without the need for full deployment. The model could also be used to predict device behaviour prior to deployment, minimizing the adjustment time required to get a device operating at full potential. There is still a significant amount of work that needs to be carried out, particularly in understanding the interaction between the non-static turbine damping and hydrodynamic response of a floating OWC. Numerical modelling of an OWC can be used in a variety of ways to tests controllers, turbines, and overall system performance, but it cannot be considered a full substitute for open sea deployment and experimentation. However, based on the data available, this model should be a useful addition to device development.

Acknowledgment

James Kelly acknowledges support from a Government of Ireland Postgraduate Research Scholarship from the Irish Research Council. The contributions of staff members at MaREI, UCC are gratefully acknowledged for preparation of this paper. The authors would like to acknowledge the results used for validation which came from research funded from the European Community's Seventh Framework Programme (FP7/2007-2013) under grant agreement no 213633 (CORES project). All research conducted by Keith O'Sullivan was completed before 01/2014, while he was working at UCC.

References

[1] A. F. de O. Falcao, "First generation wave power plants: Current status and R&D requirements", in *ASME 2003 22nd Int. Conf. Offshore Mechanics and Arctic Engineering*, pp. 723-731. American Society of Mechanical Engineers, 2003.

[2] Heath, T. V. "A review of oscillating water columns." *Philosophical Trans. Royal Society A: Mathematical, Physical and Engineering Sciences*, vol. 370, no. 1959, 2012, pp. 235-245.

[3] Y. Torre-Enciso, I. Ortubia, L. I. L. de Aguileta, and J. Marques, "Mutriku wave power plant: from the thinking out to the reality." in *Proc. 8th EWTEC Conf.*, Uppsala, Sweden, 2009, pp. 319-329.

[4] F. Paparella, K. Monk, V. Winands, M. F. P. Lopes, D. Conley, and J. V. Ringwood. "Up-Wave and Autoregressive Methods for Short-Term Wave Forecasting for an Oscillating Water Column." *IEEE Trans. on Sustainable Energy*, vol. 6, no. 1, pp. 171-178, 2015.

[5] N. Delmonte, D. Barater, F. Giuliani, P. Cova, and G. Buticchi, "Oscillating water column power conversion: A technology review", in *IEEE Energy Conversion Congress and Exposition*, Pittsburgh, PA, 2014, pp. 1852-1859.

[6] D.L. O'Sullivan, and A.W. Lewis, "Generator Selection and Comparative Performance in Offshore Oscillating Water Column Ocean Wave Energy Converters," *IEEE Trans. on Energy Conversion*, vol.26, no.2, pp.603-614, June 2011.

[7] D. Cashman, D. O'Sullivan, M. Egan, and J. Hayes, "Modelling and analysis of an offshore oscillating water column wave energy converter." in *Proc. 8th EWTEC Conf.*, Uppsala, Sweden, 2009, pp. 924-933.

[8] K. O'Sullivan and J. Murphy, "Numerical hydrodynamic and structural analysis of a floating OWC at three Irish Sites.", *Proc. 33th Int. Conf. on Ocean, Offshore, and Arctic Engineering*, San Francisco, CA, USA, 2014.

[9] W. Sheng, R. Alcorn, and A. Lewis, "Assessment of primary energy conversions of oscillating water columns. I. Hydrodynamic analysis." *Journal of Renewable and Sustainable Energy*, vol. 6, no. 5, 2014.

[10] W. Sheng, R. Alcorn, and A. Lewis, "Assessment of primary wave energy conversions of oscillating water columns. II. Power take-off and validations", *Journal of Renewable and Sustainable Energy*, vol. 6, no. 6, 2014.

[11] D. Bull and E. Johnson, "Optimal Resistive Control Strategy for a Floating OWC Device", in *Proc. 10th EWTEC Conf.*, Aalborg, Denmark, 2013.

[12] A. Thakker and F. Hourigan, "Modeling and scaling of the impulse turbine for wave power applications", *Renewable Energy*, vol. 29, no. 3. 2004, pp. 305-317.

[13] M. Amundarain, M. Alberdi, A.J. Garrido, and I. Garrido, "Modeling and Simulation of Wave Energy Generation Plants: Output Power Control," *IEEE Trans. on Industrial Electronics*, vol.58, no.1, pp.105-117, Jan. 2011.

[14] Min-Fu Hsieh, I-Hsien Lin, D.G. Dorrell, Ming-June Hsieh, and Chi-Chien Lin, "Development of a Wave Energy Converter Using a Two Chamber Oscillating Water Column," *IEEE Trans. on Sustainable Energy*, vol.3, no.3, pp.482-497, July 2012.

[15] D.L. O'Sullivan, and A.W. Lewis, "Generator Selection and Comparative Performance in Offshore Oscillating Water Column Ocean Wave Energy Converters," *IEEE Trans. on Energy Conversion*, vol.26, no.2, pp.603-614, June 2011

[16] E. Tedeschi, and M. Santos-Mugica, "Modeling and Control of a Wave Energy Farm Including Energy Storage for Power Quality Enhancement: the Bimep Case Study," *IEEE Trans. on Power Systems*, vol.29, no.3, pp.1489-1497, 2014.
[17] P.B. Garcia-Rosa, J.P. Vilela, S. Cunha, F. Lizarralde, S. F. Estefen, I.R. Machado, and E.H. Watanabe. "Wave-to-Wire Model and Energy Storage Analysis of an Ocean Wave Energy Hyperbaric Converter", *IEEE Journal of Oceanic Engineering*, vol. 39, no. 2, pp. 386-397, 2014.
[18] A. Blavette, D. L. O'Sullivan, R. Alcorn, T. W. Lewis, and M. G. Egan, "Impact of a medium-size wave farm on grids of different strength levels", *IEEE Trans. on Power Systems*, vol. 29, no. 2, 917-923, 2014.
[19] D.B. Murray, J.G. Hayes, D.L. O'Sullivan, M.G. Egan, "Supercapacitor Testing for Power Smoothing in a Variable Speed Offshore Wave Energy Converter," *IEEE Journal of Oceanic Engineering*, vol.37, no.2, pp.301-308, April 2012.
[20] S. Ceballos, J. Rea, E. Robles, I. Lopez, J. Pou, and D. O'Sullivan. "Control strategies for combining local energy storage with wells turbine oscillating water column devices." *Renewable Energy*, vol. 83, pp. 1097-1109, 2015.
[21] CORES 213633. (2011). Final Publishable Summary Report. Available: http://www.fp7-cores.eu/CORES%20Final%20publishable%20summary%20report.pdf
[22] D.V. Evans, "Wave-power absorption by systems of oscillating surface pressure distributions", *Journal of Fluid Mechanics*, vol. 114, pp. 481-499, 1982.
[23] A.J.N.A. Sarmento and A.F. de O. Falcão, "Wave generatrion by an oscillating surface-pressure and its application in wave-energy extraction", *Journal of Fluid Mechanics*, vol. 150, pp. 467-485, 1985.
[24] J. Falnes, *Ocean waves and oscillating systems*, New York: Cambridge University Press, 2002.
[25] *WAMIT v6.4*, WAMIT, Inc., Chestnut Hill, MA, 2014.
[26] B. G. Cahill, and T. Lewis, "Wave energy resource characterisation of the atlantic marine energy test site", *International Journal of Marine Energy*, vol. 1, pp. 3-15, 2013
[27] V. Venugopal, T. Davey, H. Smith, G. Smith, B. Holmes, S. Barrett, M. Prevosto, C. Maisondieu, L. Cavaleri, L. Bertotti, J. Lawrence, and F. Girard. (2011) EquiMar. Deliverable D2. 2. Wave and tidal resource characterization. Available: http://archimer.ifremer.fr/doc/00250/36152/34706.pdf
[28] S. Barrett and A. W. Lewis, "Ireland's ¼ Scale Wave Energy Test Site", *Poster presented at AGMET Conference*, Dublin, Ireland, February 2008.
[29] R. Alcorn, W. Beattie, R. Douglas, "Transient Performance Modelling of a Wells Turbine", in *Proc. 10th EWTEC Conf.*, Patras, Greece, 1998, Vol.1 pp 80-87.
[30] A. J. N. A. Sarmento, L. M. C. Gato, and A. F. de O. Falcao, "Turbine-controlled wave energy absorption by oscillating water column devices," *Ocean Engineering*, vol. 17, no. 5, pp. 481–497, 1990.
[31] C. Josset and A. H. Clement, "A time-domain numerical simulator for oscillating water column wave power plants", *Renewable Energy*, vol. 32, no. 8, pp. 1379–1402, 2007
[32] W. Sheng, R. Alcorn, A. Lewis, "On thermodynamics in the primary power conversion of oscillating water column wave energy converters", *Journal of Renewable and Sustainable Energy*, vol. 5, no. 2, 2013.
[33] W. Sheng, F. Thiebaut, M. Babuchon, J. Brooks, A. Lewis, and R. Alcorn, "Investigation to air compressibility of oscillating water column wave energy converters", *Proc. ASME 2011 30th Int. Conf. Ocean, Offshore and Arctic Engineering*, Nantes, France, 2013.
[34] C. Xiong, and Z. Liu, "Numerical analysis on impulse turbine for OWC wave energy conversion", in *IEEE Asia-Pacific Power and Energy Engineering Conference (APPEEC)*,Wuhan, China, 2011, pp. 1-5.
[35] A. Thakker, J. Jarvis, and A. Sahed, "Design charts for impulse turbine wave energy extraction using experimental data", *Renewable Energy*, vol. 34, no. 10, 2009, pp. 2264-2270.
[36] F.A. Di Bella, and P. Lorenz, "The development of a Lagrangian dynamics model of an oscillating water column (OWC), wave energy converter (WEC)," in *Oceans - St. John's, 2014* , vol., no., pp.1-9, IEEE, 14-19 Sept. 2014
[37] D. Ramirez, J.P. Bartolome, S. Martinez, L.C. Herrero, and M. Blanco, "Emulation of an OWC Ocean Energy Plant with PMSG and Irregular Wave Model," *IEEE Trans. on Sustainable Energy*, vol. PP, no.99, pp.1-9.
[38] F. Thiebaut, D. O'Sullivan, P. Kracht, S. Ceballos, J. Lopez, C. Boake, J. Bard, N. Brinquete, J. Varandas, L. M. C. Gato, R. Alcorn, and A. Lewis, "Testing of a floating OWC device with movable guide vane impulse turbine power take-off", *Proc.9th European Wave and Tidal Energy Conf.*, Southampton, United Kingdom, 2011.

James F. Kelly holds a Masters in Engineering (major: Sustainable Energy) from University College Cork, Ireland, and a Bachelors in Electrical Engineering from the University of Pittsburgh, USA. He is currently a PhD candidate in Electrical Engineering at University College Cork, Ireland, where he worked as a research engineer from 2009-2011 before beginning his PhD. His thesis focuses on real-time monitoring and control of ocean energy converters.

Dr. William M. D. Wright received his BEng and PhD degrees in engineering from the University of Warwick, England in 1991 and 1996, respectively. He continued to work there as a postdoctoral researcher until 1997, when he joined the School of Engineering in University College Cork, Ireland where he is currently Senior Lecturer in Mechanical Engineering. His research interests include ultrasonic sensors, non-contact measurement applications, signal processing and ultrasonic flow metering. He is a member of the Acoustical Society of America, a Senior Member of the IEEE and Associate Editor of IEEE Trans. UFFC.

Dr. Keith O' Sullivan received his BEng, MEngSc and PhD degrees in engineering from University College Cork, Ireland and is a member of professional body Engineers Ireland. He worked on the EU FP7 MARINA Platform project on the conceptual design and analysis of hybrid wind-wave energy platforms at the Hydraulics and Maritime Research Centre (HMRC) for which he received his PhD. Keith joined multi-national engineering consultancy company Black & Veatch in 2014 as a marine energy engineer and works both directly and indirectly with device developers of all stages of maturity on device performance and testing.

Dr. Wanan Sheng received his PhD degrees in aerospace engineering at University of Glasgow (UK) 2004, and MEng in marine hydrodynamics and test techniques from China Naval Academy in 1990, and BSc in Physics from Jiangxi Normal University (China). He is a senior research fellow at University College Cork, Ireland, since 2009 in offshore renewable energy conversion and technology development. He is the UCC PI in one FP7 project, and involved with several other EU projects and national projects in wave energy conversion and optimization of the wave energy devices. He is a member of scientific committee for OMAE, ISSC V4 and RENEW.